Ultrasound in Med. & Biol., Vol. 43, No. 5, pp. 967–973, 2017

0301-5629/$ - see front matter

http://dx.doi.org/10.1016/j.ultrasmedbio.2017.01.010

● *Original Contribution*

EFFECT OF HYPOXEMIA ON FETAL VENTRICULAR DEFORMATION IN A CHRONICALLY INSTRUMENTED SHEEP MODEL

Amarnath Bhide,* Juha Rasanen,[†‡§] Heikki Huhta,[§] Juulia Junno,[§] Tiina Erkinaro,[¶] Pasi Ohtonen,[‖] Mervi Haapsamo,[#] and Ganesh Acharya[**]

*Women's Health & Perinatal Research Group, Department of Clinical Medicine, UiT—The Arctic University of Norway, Tromsø, Norway; [†]Department of Obstetrics and Gynecology, Kuopio University Hospital and University of Eastern Finland, Kuopio, Finland; [‡]Department of Obstetrics and Gynecology, Helsinki University Hospital, Helsinki, Finland; [§]Department of Obstetrics and Gynecology, Oulu University Hospital, Oulu, Finland; [¶]Department of Anaesthesiology, Oulu University Hospital, Oulu, Finland; [‖]Department of Statistics, Oulu University Hospital, Oulu, Finland; [#]Department of Obstetrics and Gynecology, Lapland Central Hospital, Rovaniemi, Finland; and **Department of Clinical Science, Intervention and Technology (CLINTEC), Karolinska Institutet, Stockholm, Sweden

(*Received* 2 *August* 2016; *revised* 1 *December* 2016; *in final form* 19 *January* 2017)

Abstract—We hypothesized that in near-term sheep fetuses, hypoxemia changes myocardial function as reflected in altered ventricular deformation on speckle-tracking echocardiography. Fetuses in 21 pregnant sheep were instrumented. After 4 d of recovery, fetal cardiac function was assessed by echocardiography at baseline, after 30 and 120 min of induced fetal hypoxemia and after its reversal. Left (LV) and right (RV) ventricular cardiac output and myocardial strain were measured. Baseline mean (standard deviation [SD]) LV and RV global longitudinal strains were −18.7% (3.8) and −14.3% (5.3). Baseline RV global longitudinal and circumferential deformations were less compared with those of the left ventricle ($p = 0.016$ and $p < 0.005$). LV, but not RV, global longitudinal strain was decreased ($p = 0.003$) compared with baseline with hypoxemia. Circumferential and radial strains did not exhibit significant changes. In the near-term sheep fetus, LV global longitudinal and circumferential strains are more negative than RV strains. Acute hypoxemia leads to LV rather than RV dysfunction as reflected by decreased deformation. (E-mail: abhide@sgul.ac.uk)

Key Words: **Speckle-tracking echocardiography, Hypoxemia, Sheep model.**

INTRODUCTION

Fetal cardiovascular protective response to moderate isocapnic hypoxemia involves chemoreflex, endocrine and local components. Acute fetal hypoxemia is associated with increased blood flow to the myocardium, brain and adrenal glands, but the fetal autonomic response to hypoxemia varies by gestational age (Iwamoto et al. 1989). At 0.6–0.7 gestation in fetal sheep (87–102 d), arterial blood pressure does not change significantly and fetal heart rate may remain unchanged or increase slightly (Iwamoto et al. 1989), whereas at 0.9 gestation, vagally mediated bradycardia and a rise in blood pressure are observed (Giussani et al. 1993). Hemodynamic changes related to acute and chronic hypoxemia in sheep fetuses have been well described (Carter 2015; Jensen et al. 1999; Rudolph 1985). Chronic hypoxemia without acidemia does not affect fetal cardiac output (Block et al. 1990). Blood flow to the placenta, carcass, kidney and spleen is maintained with chronic hypoxemia until fetal acidosis develops (Jensen et al. 1999). We have reported that acute hypoxemia in near-term fetal sheep leads to an increase in pulmonary arterial vascular impedance and an increase in right ventricular cardiac output (Mäkikallio et al. 2006). Peak myocardial velocities measured by tissue Doppler technique appear to decrease during hypoxemia/acidemia, especially during isovolumic periods of the cardiac cycle (Acharya et al. 2008). However, changes in myocardial strain that may occur during fetal hypoxemia have not been elucidated.

Two-dimensional strain imaging uses standard B-mode images and speckle tracking for evaluation of myocardial deformation. Lagrangian strain is defined as the instantaneous lengthening or shortening compared with initial muscle fiber length, which, in the myocardium, is commonly determined by the end of diastole

Address correspondence to: Amarnath Bhide, Fetal Medicine Unit, 4th Floor, Lanesborough Wing, St. George's Hospital, Blackshaw Road, SW17 0 QT, UK. E-mail: abhide@sgul.ac.uk

(D'Hooge et al. 2000). The relative independence of the angle of the ultrasound beam and direction of movement makes this technique less vulnerable to errors. Speckle-tracking echocardiography is still a research tool, and its value in clinical practice is under debate (Huang and Orde 2013; Orde et al. 2016; Tanaka and Hirata 2016). This technique has been used to evaluate cardiac function in normal fetuses (Kapusta et al. 2012), fetuses of diabetic mothers (Kulkarni et al. 2016), fetuses with twin-to-twin transfusion syndrome and those with congenital diaphragmatic hernia (Van Mieghem et al. 2011). To our knowledge, the response of fetal myocardium to hypoxemia has not been evaluated using speckle-tracking echocardiography.

The present experiment in near-term fetal sheep was designed to test the hypothesis that a decrease in fetal oxygenation leads to compensatory changes in myocardial function that can be detected by 2-D speckle-tracking echocardiography. Specifically, we asked two questions in this study: (i) Are left and right ventricular deformations similar under normoxemic conditions? (ii) Are the responses of left and right ventricular deformations to prolonged hypoxemia different?

METHODS

All experiments were performed in accordance with the European Convention for the Protection of Vertebrate Animals Used for Experimental and Other Scientific Purposes (Council of Europe 1986) and European Union Directive ETS 123 (1997). The Animal Care and Use Committee of the University of Oulu approved the study protocol.

Data from 21 chronically instrumented pregnant sheep were used for this report. Mean (standard deviation [SD]) weights of the ewes and the fetuses were 53.9 (8.1) kg and 2401 (256) g, respectively.

Surgery was performed at 115–129 gestational d (term: 145 d). Ewes were fasted overnight and premedicated with intra-muscular ketamine (2 mg/kg) and midazolam (0.2 mg/kg). The maternal external jugular vein was cannulated, and Ringer's lactate solution was infused at a rate of 200 mL/h. General anesthesia was induced with intra-venous propofol (4–7 mg/kg) and maintained with isoflurane (1.5–2.5%) in an oxygen–air mixture delivered *via* an endotracheal tube. Intravenous boluses of fentanyl (0.05–0.15 mg) were administered as required.

A laparotomy was performed under general anesthesia and endotracheal intubation. The fetal head and neck were delivered through a small uterine incision. Catheters were introduced into the internal jugular vein and carotid artery to allow access to arterial and venous circulations and to collect blood samples.

A small left lateral thoracotomy was performed at the level of the third intercostal space, and the ductus arteriosus was identified and dissected. A 4-mm ultrasonic transit-time flow probe was secured around the vessel and tunneled outside for measurement of ductus arteriosus blood flow. Thoracotomy was closed. Electrocardiogram leads were placed subcutaneously to obtain fetal electrocardiogram. A catheter was anchored to the fetal skin to measure intra-amniotic pressure. After replacement of amniotic fluid with 0.9% warm saline and closure of the surgical wounds, all catheters and probes were tunneled subcutaneously and exteriorized through a small skin incision in the ewe's flank. Post-operative analgesia was provided with a fentanyl patch (50 μg/h) attached to the ewe's tail, with additional intra-muscular injections of fentanyl 1.5 to 2 mg/kg twice daily.

After a 4-d recovery, general anesthesia was induced again as described above. A 16-gauge polyurethane catheter was inserted into the maternal descending aorta through a femoral artery. The ewe was placed supine with a right lateral tilt and allowed to stabilize for 30 min before the baseline measurements were taken. Thereafter, maternal and fetal hypoxemia was induced by replacing inhaled oxygen with medical air in the re-breathing circuit to reach a maternal oxyhemoglobin saturation level of 75%–80%. Hypoxemia phase data were obtained 30 and 120 min after reaching the desired maternal saturation level. After data collection for the last hypoxemia phase was completed, oxygen was substituted and re-breathing was discontinued to allow recovery from hypoxemia. Recovery phase data were obtained 15 min after maternal normoxemia was established. Fetal heart rate was monitored with a cardiotachometer triggered from the arterial pressure waves. Fetal arterial blood pressure was referenced to amniotic fluid pressure. Fetal blood samples were obtained to measure acid–base status and blood gases at the end of each phase. At the end of the experiment, animals were euthanized with an intravenous overdose (1.0 mg/kg) of pentobarbital sodium. Fetal weight was recorded.

Fetal echocardiography was performed using the Vivid 7 ultrasound system (GE Medical Systems, Horten, Norway) with a 10-MHz phased-array transducer to obtain 2-D gray-scale images with a high frame rate. Cine-loop images of four-chamber and short-axis views at the level of papillary muscles were obtained by a single investigator (J.R.). The imaging depth was 5–10 cm, and the mechanical index and thermal index were kept below 1.5 and 1.0, respectively. Two stable well-defined consecutive cardiac cycles from each view were used for speckle-tracking analysis. The scan-line digital data for these images were processed using acoustic-tracking software (EchoPAC, GE Medical Systems), allowing off-line semi-automated analysis of speckle-based strain.

The off-line analysis was performed by a single operator (A.B.) who was blinded to fetal arterial blood gas values and hemodynamic data. The endocardial surface was manually traced at the end-systolic frame, and an automated tracking algorithm outlined the myocardium in successive frames throughout the cardiac cycle (Fig. 1). Tracking quality was verified automatically for each segment. Manual adjustment of the region of interest was performed if necessary. Myocardial global longitudinal strain was measured for the left and right ventricles on a four-chamber view. These measurements were repeated in another cardiac cycle from the second stored cine loop of the same fetus. The mean of these two measurements was used for data analysis. The inter-ventricular septum was not excluded while measurement of the RV global longitudinal strain was performed. Global circumferential and radial strains for the left and the right ventricle (Hayabuchi et al. 2015) were calculated from the short-axis view at the level of the papillary muscles (Fig. 2). An average of segmental values was calculated to obtain global values.

Blood flow velocity waveforms were obtained at the level of aortic and pulmonary valves, while keeping the angle of insonation close to zero degrees (always $<15°$), and the mean velocities were determined (mean velocity = time−velocity integral × heart rate). Inner diameters of the aortic and pulmonary valves were measured using B-mode cine-loop images while keeping the insonation angle perpendicular to the vessels as far as possible (Kiserud et al. 2006). An average of three measurements was used for calculating cardiac outputs. Left (LVCO) and right (RVCO) ventricular cardiac outputs were computed separately as cardiac output (CO) = mean velocity × 3.14 (diameter of the outflow tract/2)^2. Combined cardiac output (CCO) was calculated as the sum of LVCO and RVCO.

Pulmonary volume blood flow was calculated as the difference between RVCO and ductus arteriosus volume blood flow. Doppler blood flow velocity waveforms were obtained from the right pulmonary artery (RPA) as described previously (Rasanen et al. 1996). Pulsatility index (PI) was calculated as (peak systolic velocity − end-diastolic velocity)/time-averaged maximum velocity (Deane 2000) as a surrogate for pulmonary arterial vascular impedance.

Data were expressed as means and SD unless stated otherwise. A linear mixed model (LMM) was used for repeatedly measured data. If the linear mixed model differed significantly between measurement points ($P_{time} < 0.05$), then a pairwise comparison between relevant points was performed. A paired sample *t*-test was used to compare LV and RV global longitudinal, circumferential and radial strains. Mean differences with 95% confidence intervals are presented for paired sample *t*-tests. Statistical analyses were performed using SPSS Statistics for Windows, Version 20.0 (IBM Armonk, NY, USA), and SAS Version 9.3 (SAS Institute, Cary, NC, USA). A two-tailed p value < 0.05 was considered to indicate statistical significance.

RESULTS

Maternal hypoxemia led to a significant reduction in fetal pO_2, which, during the recovery phase, returned to baseline level (Table 1). Fetal pH decreased significantly at the 120 min hypoxemia phase and remained significantly lower during the recovery phase than at baseline. In addition, fetal lactate level was significantly

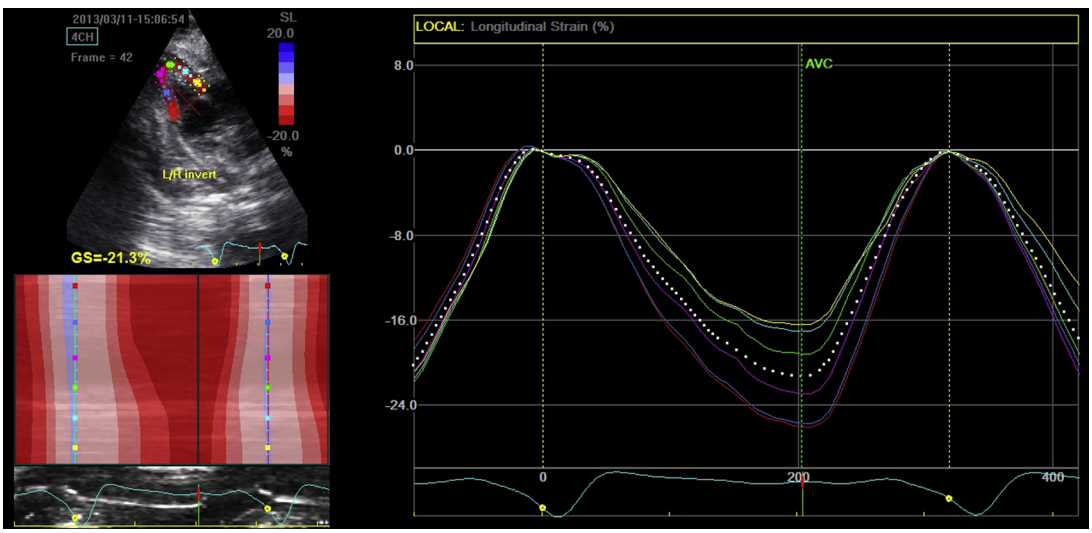

Fig. 1. Automated tracking algorithm outlining the myocardium and calculation of global strain and strain rate using Echopac software.

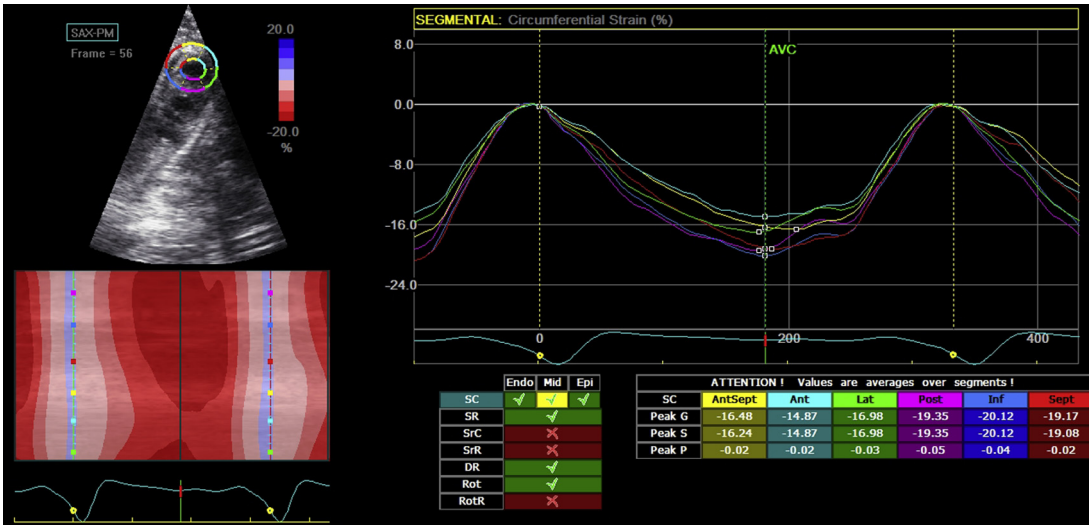

Fig. 2. Automated tracking algorithm outlining the myocardium and calculation of right ventricular global circumferential strain using Echopac software.

higher during the hypoxemia and recovery phases than at baseline. Fetal pCO_2 did not change during the experiment. Hypoxemia decreased fetal arterial blood pressures significantly (Table 1). Fetal heart rate was significantly lower at the recovery phase compared with the baseline and hypoxemia phases. During hypoxemia, there was a significant increase in fetal RPA PI values and a decrease in LVCO. Pulmonary blood flow decreased with hypoxemia compared with baseline, but the reduction did not reach statistical significance. Fetal RVCO and CCO remained stable during the entire experiment (Table 1).

2-D strain data

Ultrasound recordings were obtained at a mean frame rate of 167 (range: 126–235) frames/s. At baseline, there was significantly more deformation in the LV global longitudinal ($p = 0.016$) and circumferential ($p < 0.005$) strains than in the corresponding RV parameters (Table 2). Hypoxemia at 30 and 120 min led to a significant reduction (less deformation) in LV global longitudinal strain, whereas the global circumferential and radial strains were not affected by fetal hypoxemia (Table 2, Fig. 3). During the recovery period, LV global longitudinal strain returned to baseline level. Right ventricular

Table 1. Fetal parameters during the experiment

Parameter	Baseline	Hypoxemia (30 min)	Hypoxemia (120 min)	Recovery	P_{time}
Fetal heart rate (beats/min)	169 (38)	166 (26)	170 (24)	136 (16)	0.004*
Fetal SBP (mm Hg)	60 (10.3)	52 (8.5)	54 (7.4)	56 (8.7)	0.0008†
Fetal DBP (mm Hg)	40 (7.5)	35 (8.8)	36 (7.3)	37 (8.4)	0.034†
Fetal MAP (mm Hg)	49 (10.7)	43 (11.2)	47 (10.9)	48 (10.3)	0.050
Fetal pO_2 (kPa)	2.79 (0.32)	1.59 (0.40)	1.49 (0.16)	2.80 (0.41)	<0.0001
Fetal pCO_2 (kPa)	6.51 (1.06)	6.68 (0.48)	7.05 (0.99)	6.81 (0.48)	0.56‡
Fetal pH	7.32 (0.05)	7.30 (0.04)	7.14 (0.12)	7.17 (0.06)	<0.0001§
Fetal base excess (mmol/mL)	−1.39 (2.35)	−2.05 (2.92)	−10.70 (6.07)	−9.63 (3.25)	<0.0001§
Fetal lactate (mM/mL)	2.42 (1.63)	4.10 (1.84)	10.17 (3.94)	9.91 (4.20)	<0.0001§
LVCO (mL/min)	644 (198)	501 (122)	545 (123)	548 (157)	0.010§
RVCO (mL/min)	644 (159)	638 (229)	651 (179)	619 (147)	0.60
CCO (mL/min)	1288 (294)	1125 (246)	1184 (240)	1158 (229)	0.19
Right pulmonary artery PI	12.54 (11.75)	66.97 (26.88)	57.08 (23.94)	69.42 (56.93)	0.006¶
Pulmonary flow (mL/min)	467 (177)	311 (127)	303 (204)	299 (179)	0.089

SBP = systolic blood pressure; DBP = diastolic blood pressure; MAP = mean arterial pressure; LVCO = left ventricular cardiac output; RVCO = right ventricular cardiac output; CCO = combined cardiac output; PI = pulsatility index.

* Fetal heart rate differed significantly with recovery compared with all other phases.

† Significant difference between baseline and 30 min hypoxemia, as well as between baseline and 120 min hypoxemia, for SBP and DBP.

‡ Significant difference between baseline and 30 and 120 min hypoxemia for pO_2.

§ Significant difference between baseline and all the other three phases for pH, LVCO, base excess and lactate.

¶ Right pulmonary artery PI was log transformed. Significant difference between baseline and 30 min hypoxemia, 120 min hypoxemia and recovery for right pulmonary artery PI.

Table 2. 2-D strain data using speckle-tracking echocardiography

Parameter	Baseline	Hypoxemia (30 min)	Hypoxemia (120 min)	Recovery	P_{time}
LV global longitudinal strain (%)*	−18.7 (3.8)†,*	−13.9 (3.3)	−15.4 (4.3)	−17.8 (2.9)	0.005†
LV global longitudinal strain rate (1/s)§	−2.50 (0.55)	−2.58 (0.64)	−2.67 (0.86)	−2.70 (0.79)	0.91
LV circumferential strain (%)‡	−21.0 (5.9)	−18.5 (6.7)	−19.3 (6.6)	−19.3 (5.7)	0.69
LV radial strain (%)	17.1 (7.0)	12.8 (6.3)	14.5 (5.4)	13.7 (4.7)	0.31
RV global longitudinal strain (%)†,*	−14.3 (5.4)†,*	−14.8 (2.7)	−14.7 (3.9)	−15.3 (2.2)	>0.9
RV global longitudinal strain rate (1/s)§	−2.00 (0.48)	−2.27 (0.50)	−2.11 (0.86)	−2.07 (0.37)	0.57
RV circumferential strain (%)‡	−11.1 (5.3)	−13.6 (5.6)	−11.7 (6.3)	−11.7 (4.6)	0.20
RV radial strain (%)	14.3 (4.8)	10.8 (2.0)	10.3 (5.1)	14.1 (4.8)	0.15

LV = left ventricular; RV = right ventricular.
* $p = 0.016$ between baseline LV and RV global longitudinal strain.
† $p = 0.0011$ between baseline and 30 min hypoxemia, $p = 0.026$ between baseline and 120 min hypoxemia and $p = 0.013$ between 30 min hypoxemia and recovery.
‡ $p < 0.005$ between baseline LV and RV circumferential strain.
§ $p = 0.003$ between baseline LV and RV global longitudinal strain rate.

global longitudinal, circumferential and radial strains did not change statistically significantly. Baseline left ventricular strain rate was significantly higher than the right rate ($p = 0.003$). There were no significant changes in left or right ventricular global longitudinal strain rates during the experiment (Table 2).

DISCUSSION

The present study was designed to investigate the effect of fetal hypoxemia on LV and RV strain formation. The experiments were done in fetal sheep at 0.8 gestation, which corresponds to approximately 30–32 wk of human gestation. Blood gas values revealed that after 30 min of hypo-oxygenation, the fetuses were hypoxemic without any significant metabolic component, but prolonged hypoxemia (120 min) led to significant fetal metabolic acidemia. In the recovery phase, fetal oxygenation returned to baseline level, but there was still significant metabolic acidemia. We found that at baseline, there was more global longitudinal and circumferential deformation (strain) in the left ventricle than in the right ventricle. Fetal hypoxemia was associated with reduced LV global longitudinal strain that returned to baseline level when

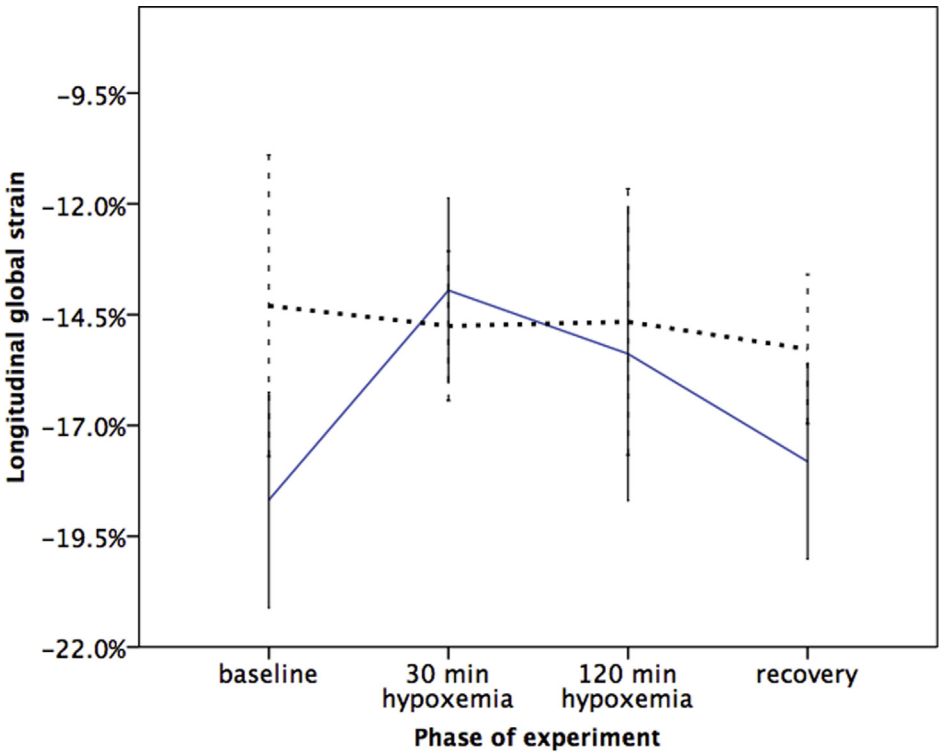

Fig. 3. Global left (*solid lines*) and right (*dotted line*) ventricular longitudinal strain with hypoxemia and recovery.

fetal normoxemia was restored, even though the fetus still had significant metabolic acidemia. Fetal hypoxemia, even with metabolic academia, had no effect on RV strains.

A reduction in LV global longitudinal deformation with hypoxemia may be a result of reduced LV preload, direct LV myocardial dysfunction or a combination of the two. It has been reported that pulmonary circulation is sensitive to fetal oxygenation during the last trimester of pregnancy (Rasanen et al. 1996) and that hypoxemia leads to pulmonary vasoconstriction (Arraut et al. 2013). Indeed, in the current experiment, RPA PI values increased significantly with hypoxemia, suggesting that impedance to pulmonary blood flow increased during hypoxemia, although the reduction in the estimated pulmonary volume blood flow was not statistically significant. It has been reported in a near-term sheep model of acute ductus arteriosus occlusion that the fetus is unable to increase volume blood flow across the foramen ovale (Tulzer et al. 1991); thus, the reduction in LVCO is most likely a consequence of a drop in pulmonary volume blood flow leading to a decrease in LV preload. It has been reported in human fetuses that global longitudinal strain is similar in both ventricles at 20–24 wk of gestation (Kapusta et al. 2012). Later in pregnancy, LV global longitudinal strain does not change; however, corresponding RV strain or deformation decreases. This is explained by an increase in the RV preload. If the change in preload was the major factor in strain formation, we should have observed an opposite finding for LV global longitudinal strain. Therefore, our results indicate that the direct effect of hypoxemia on intrinsic contractile properties of the left ventricle is likely responsible for decreased global longitudinal strain.

Fetal global LV longitudinal deformation had already decreased at 30 min of hypoxemia, when significant metabolic acidemia had not yet developed. At 120 min of hypoxemia, fetal pO_2 was comparable to that at 30 min of hypoxemia; however, significant metabolic acidemia had developed between these two points. Interestingly, we found no further deterioration in any of the strain parameters. We previously reported that the fetal left ventricle is more susceptible to hypoxemia compared with the fetal right ventricle. However, in that study, fetal cardiac function and hemodynamics were assessed by tissue Doppler and pulsed Doppler imaging, rather than speckle tracking. The findings of this study corroborate our previous observations. We also found that the fetal LV myocardial performance index significantly worsens with hypoxemia (Bhide et al. 2016), which also supports the findings of this study. At the recovery phase, when fetal oxygenation returned to baseline conditions, LV global longitudinal strain values were similar to baseline values, even though fetuses still had significant metabolic acidemia. Furthermore, LVCO, RVCO or CCO did not exhibit significant changes with progressive metabolic acidemia. This indicates that fetal myocardial function had not further deteriorated despite worsening metabolic acidemia. Our results suggest that LV function is more sensitive to oxygenation than metabolic acidosis. Experimental intra-venous infusion of lactic acid into sheep fetuses led to a reduction in fetal pH and increase in heart rate but no change in blood pressure (Hohimer and Bissonnette 1991). This also suggests that lactic acid does not influence cardiac function.

Di Salvo et al. (2005) were the first to describe fetal LV and RV function using ultrasound-based strain and strain rate imaging. They used myocardial color Doppler imaging for quantification of strain. Doppler technology is known to be angle dependent, which speckle tracking can eliminate (Biswas et al. 2013). Several software programs assess myocardial deformation using speckle tracking. However, they are not necessarily comparable. Velocity vector imaging mainly tracks myocardial motion in a narrow area just underneath the endocardium. In contrast, EchoPAC automated functional imaging software tracks myocardial deformation in a relatively wider area, specified by the operator (Biswas et al. 2013).

Strengths and weaknesses

A rate of at least 60–110 frames per second is recommended when imaging the adult heart (Mondillo et al. 2011), and even higher rates are desirable to provide enough frames per heartbeat in the fetus (Matsui et al. 2011). We studied the fetus at a mean frame rate of 167 Hz, and this is likely to have led to reliable results. The surgical procedures may constitute a significant stress on the sheep fetuses, and it may be argued that the conditions are quite different from those of human fetuses exposed to hypoxemia. Normal arterial blood gas values at the baseline stage suggest conditions close to physiologic circulatory state (Acharya et al. 2004). The study was carried out in a narrow gestational age window of 115–129 d, which may limit validity and significance outside this period.

These results should be extrapolated to human pregnancy cautiously. The sheep model has been extensively used for research in fetal hemodynamics, and the myocardial strain curves are similar in normal ovine and human pregnancy. We did not monitor cerebral blood flow during the experiment, and it could be argued that the reduction in LV global longitudinal strain may simply reflect a drop in cerebral vascular resistance during hypoxemia. Indeed, carotid artery blood pressure decreased during hypoxemia. Furthermore, it has been reported that carotid artery volume blood flow increases from about 85 mL/min (normoxemia) to about 95–100 mL/min during isocapnic hypoxemia (Bennet et al. 1998). We can estimate that

there was an approximately 24% reduction in carotid artery vascular resistance during hypoxemia. However, based on these estimations, more than 80% of LVCO bypasses brain circulation during prolonged hypoxemia and is affected by lower body vascular resistance. Thus, we believe that reduced carotid artery vascular resistance is not the main determinant of reduced LV global longitudinal strain during hypoxemia.

CONCLUSIONS

We have found that hypoxemia leads to changes in fetal cardiac function that are reflected in altered ventricular deformation on speckle-tracking echocardiography. At a gestational age equivalent to 0.8 term, the global longitudinal and circumferential strains are less negative in the right than in the left ventricle. The fetus responds to acute hypoxemia by reduced deformation of the left but not the right ventricle, and this response is reversed by reversal of hypoxemia. This recovery of LV function is seen even in the presence of metabolic acidemia.

Acknowledgments—This study was funded by the Regional Health Authority of Northern Norway (Project No. 12050).

REFERENCES

Acharya G, Erkinaro T, Makikallio K, Lappalainen T, Rasanen J. Relationships among Doppler-derived umbilical artery absolute velocities, cardiac function, and placental volume blood flow and resistance in fetal sheep. Am J Physiol Heart Circ Physiol 2004; 286:H1266–H1272.

Acharya G, Rasanen J, Makikallio K, Erkinaro T, Kavasmaa T, Haapsamo M, Mertens L, Huhta JC. Metabolic acidosis decreases fetal myocardial isovolumic velocities in a chronic sheep model of increased placental vascular resistance. Am J Physiol Heart Circ Physiol 2008;294:H498–H504.

Arraut AM, Frias AE, Hobbs TR, McEvoy C, Spindel ER, Rasanen J. Fetal pulmonary arterial vascular impedance reflects changes in fetal oxygenation at near-term gestation in a nonhuman primate model. Reprod Sci 2013;20:33–38.

Bennet L, Peebles DM, Edwards AD, Rios A, Hanson MA. The cerebral hemodynamic response to asphyxia and hypoxia in the near-term fetal sheep as measured by near infrared spectroscopy. Pediatr Res 1998;44:951–957.

Bhide A, Vuolteenaho O, Haapsamo M, Erkinaro T, Rasanen J, Acharya G. Effect of hypoxemia with or without increased placental vascular resistance on fetal left and right ventricular myocardial performance index in chronically instrumented sheep. Ultrasound Med Biol 2016;42:2589–2598.

Biswas M, Sudhakar S, Nanda NC, Buckberg G, Pradhan M, Roomi AU, Gorissen W, Houle H. Two- and three-dimensional speckle tracking echocardiography: Clinical applications and future directions. Echocardiography 2013;30:88–105.

Block BS, Schlafer DH, Wentworth RA, Kreitzer LA, Nathanielsz PW. Intrauterine asphyxia and the breakdown of physiologic circulatory compensation in fetal sheep. Am J Obstet Gynecol 1990;162: 1325–1331.

Carter AM. Placental gas exchange and the oxygen supply to the fetus. Compr Physiol 2015;5:1381–1403.

D'Hooge J, Heimdal A, Jamal F, Kukulski T, Bijnens B, Rademakers F, Hatle L, Suetens P, Sutherland GR. Regional strain and strain rate measurements by cardiac ultrasound: principles, implementation and limitations. Eur J Echocardiogr 2000;1:154–170.

Deane C. Doppler ultrasound: Principles and practice. In: Niclaides K, Rizzo G, Hecher K, (eds). Placental and fetal Doppler. London: Parthenon; 2000. p. 22.

Di Salvo G, Russo MG, Paladini D, Pacileo G, Felicetti M, Ricci C, Cardaropoli D, Palma M, Caso P, Calabro R. Quantification of regional left and right ventricular longitudinal function in 75 normal fetuses using ultrasound-based strain rate and strain imaging. Ultrasound Med Biol 2005;31:1159–1162.

Giussani DA, Spencer JA, Moore PJ, Bennet L, Hanson MA. Afferent and efferent components of the cardiovascular reflex responses to acute hypoxia in term fetal sheep. J Physiol 1993;461:431–449.

Hayabuchi Y, Sakata M, Kagami S. Right ventricular myocardial deformation patterns in children with congenital heart disease associated with right ventricular pressure overload. Eur Heart J Cardiovasc Imaging 2015;16:890–899.

Hohimer AR, Bissonnette JM. Vascular lactic acid infusions do not alter the incidence of fetal breathing movements or their inhibition by acute hypoxemia. Pediatr Res 1991;29:483–486.

Huang SJ, Orde S. From speckle tracking echocardiography to torsion: Research tool today, clinical practice tomorrow. Curr Opin Crit Care 2013;19:250–257.

Iwamoto HS, Kaufman T, Keil LC, Rudolph AM. Responses to acute hypoxemia in fetal sheep at 0.6–0.7 gestation. Am J Physiol 1989; 256:H613–H620.

Jensen A, Garnier Y, Berger R. Dynamics of fetal circulatory responses to hypoxia and asphyxia. Eur J Obstet Gynecol Reprod Biol 1999; 84:155–172.

Kapusta L, Mainzer G, Weiner Z, Deutsch L, Khoury A, Haddad S, Lorber A. Second trimester ultrasound: Reference values for two-dimensional speckle tracking-derived longitudinal strain, strain rate and time to peak deformation of the fetal heart. J Am Soc Echocardiogr 2012;25:1333–1341.

Kiserud T, Ebbing C, Kessler J, Rasmussen S. Fetal cardiac output, distribution to the placenta and impact of placental compromise. Ultrasound Obstet Gynecol 2006;28:126–136.

Kulkarni A, Li L, Craft M, Nanda M, Lorenzo JM, Danford D, Kutty S. Fetal myocardial deformation in maternal diabetes mellitus and obesity. Ultrasound Obstet Gynecol 2016; http://dx.doi.org/10.1002/uog.15971 [Epub ahead of print.].

Mäkikallio K, Erkinaro T, Niemi N, Kavasmaa T, Acharya G, Päkkilä M, Räsänen J. Fetal oxygenation and Doppler ultrasonography of cardiovascular hemodynamics in a chronic near-term sheep model. Am J Obstet Gynecol 2006;194:542–550.

Matsui H, Germanakis I, Kulinskaya E, Gardiner HM. Temporal and spatial performance of vector velocity imaging in the human fetal heart. Ultrasound Obstet Gynecol 2011;37:150–157.

Mondillo S, Galderisi M, Mele D, Cameli M, Lomoriello VS, Zacà V, Ballo P, D'Andrea A, Muraru D, Losi M, Agricola E, D'Errico A, Buralli S, Sciomer S, Nistri S, Badano L. Echocardiography Study Group of the Italian Society of Cardiology (Rome, Italy). Speckle-tracking echocardiography: A new technique for assessing myocardial function. J Ultrasound Med 2011;30:71–83.

Orde S, Huang SJ, McLean AS. Speckle tracking echocardiography in the critically ill: Enticing research with minimal clinical practicality or the answer to non-invasive cardiac assessment? Anaesth Intensive Care 2016;44:542–551.

Rasanen J, Wood DC, Weiner S, Ludomirski A, Huhta JC. Role of the pulmonary circulation in the distribution of human fetal cardiac output during the second half of pregnancy. Circulation 1996;94: 1068–1073.

Rudolph AM. Distribution and regulation of blood flow in the fetal and neonatal lamb. Circ Res 1985;57:811–821.

Tanaka H, Hirata K. Is speckle tracking actually helpful for cardiac resynchronization therapy? J Echocardiogr 2016;14:53–60.

Tulzer G, Gudmundsson S, Rotondo KM, Wood DC, Yoon GY, Huhta JC. Acute fetal ductal occlusion in lambs. Am J Obstet Gynecol 1991;165:775–778.

Van Mieghem T, Deprest J, Verhaeghe J. Fetal and maternal hemodynamics in pregnancy: New insights in the cardiovascular adaptation to uncomplicated pregnancy, twin-to-twin transfusion syndrome and congenital diaphragmatic hernia. Facts Views Vis Obgyn 2011;3: 205–213.